RC22394 (W0204-051) April 11, 2002
Materials Science

IBM Research Report

Observaton and Modelling of the Transient Fast Interdiffusion Regime in Si/SiGe Superlattices

D.B. Aubertine, M.A. Mander, N. Ozguven, A.F. Marshall, P.C. McIntyre
Department of Materials Science and Engineering
Stanford University, Stanford, CA

P.M. Mooney , J.O. Chu
IBM Research Division
Thomas J. Watson Research Center
P.O. Box 218
Yorktown Heights, NY 10598

Research Division
Almaden - Austin - Beijing - Delhi - Haifa - India - T. J. Watson - Tokyo - Zurich

Observation and Modelling of the Transient Fast Interdiffusion Regime in Si/SiGe Superlattices

D.B. Aubertine, M.A. Mander, N. Ozguven, A.F. Marshall and P.C. McIntyre

Department of Materials Science and Engineering
Stanford University, Stanford, CA

P.M. Mooney and J.O. Chu

IBM Research Division
T.J. Watson Research Center, Yorktown Heights, NY

X-ray diffraction is used to probe interdiffusion in asymmetrically strained, low concentration Si/SiGe superlattices. The results are shown to be in good agreement with a model developed from literature data for Ge diffusion in SiGe alloys obtained by an entirely different measurement strategy. Using this model it is shown that the transient fast diffusion frequently observed in Si/SiGe superlattices results primarily from the concentration dependence of the activation enthalpy for SiGe interdiffusion. Time dependent strain relaxation is shown to play a discernible, but secondary role in the transition from fast to slow diffusion. The linear proportionality constant relating the activation enthalpy of SiGe interdiffusion to biaxial strain is found to be ~19 eV/unit strain.

I Introduction

Silicon germanium occupies an important place in the scheme of modern semiconductor technology. As opposed to pure Si, SiGe alloys offer adjustable bandgaps, enhanced carrier mobility and a higher dopant solubility. For high speed applications, its properties are competitive with III-V alloys and its compatibility with Si processing makes it considerably less expensive to integrate with Si-based technologies. There are, however, two key materials issues limiting the usefulness of SiGe – interdiffusion and strain relaxation. While both processes have been extensively studied, the degree to which they are coupled remains an open question.

It has been frequently observed that SiGe interdiffusion exhibits a fast, transient regime, followed by slower, steady state behavior. [1–4] The explanations given for this behavior often focus on a coupling with time-dependent strain relaxation processes.[1,5,6] For example, Iyer and LeGoues[1] suggested that rapid interdiffusion kinetics observed in experiments on coherent $Si_{0.88}Ge_{0.12}$/Si multilayers were caused by the biaxial compressive strain present in the SiGe layers. They suggested that dislocation-mediated strain relaxation during annealing of initially-dislocated multilayers reduced the driving force for interdiffusion, resulting in much slower diffusion kinetics than observed for coherent multilayers. Other proposed causes include a strong dependence of interdiffusivity on Ge concentration[3,7] , additional diffusivity caused by a strain potential gradient,[8] and annihilation of an initial non-equlibrium point defect concentration.[4,9] Based on the work presented here, we attribute the transient, fast diffusion to a combination of two of these effects – the dependence of interdiffusion's acti-

vation enthalpy on concentration and on strain. Experiments in both bulk SiGe and relaxed SiGe films have shown that the activation enthalpy for SiGe interdiffusion depends separately on strain and concentration.[10,11] This idea also follows naturally from the known difference in activation energies for self diffusion in the unstrained, bulk materials – 4.5 eV in Si[12] and 3.1 eV in Ge.[13] Theoretical work by Aziz has shown that the activation enthalpy for diffusion in a biaxially strained media should be, to first order, linearly proportional to biaxial strain.[14]

$$\Delta H_a\,(net) = \Delta H_a + Q'\varepsilon_{biaxial} \tag{1}$$

To obtain meaningful values for Q' and $\Delta H_a(\mathrm{X}_{Ge})$ the effects of strain and concentration must be separated experimentally. Studies that separate strain and concentration effects have been performed with good success for B[15] and Sb[16,17] diffusion in Si and for interdiffusion in InGaAl.[18] Several authors have made similar investigations of SiGe, but the conclusions drawn from these studies have been inconsistent. Cowern et al.[19,20] compared interdiffusion in relaxed Si, Si strain in biaxial tension, relaxed $Si_{0.7}Ge_{0.3}$, and compressively strained $Si_{0.7}Ge_{0.3}$. From these four data points, they extracted values for Q'(compressive), Q'(tensile), and a linear concentration dependence for the activation enthalpy. Zangenberg et al.[10] measured Ge self-diffusion in a series of fully relaxed SiGe films ranging in concentration from 10% to 50% Ge. They extracted a highly non-linear dependence of the activation enthalpy on X_{Ge}. By adjusting the concentration of their SiGe buffer layers, they also measured diffusion rates in compressively and tensily strained $Si_{0.9}Ge_{0.1}$. From these two data, points they extrapolated values for Q'(compressive) and Q'(tensile). Both McVay et al.[11] and Strohm et al.,[13] working with polycrystalline bulk SiGe and relaxed SiGe films respec-

tively, also found a highly non-linear concentration dependence of the activation enthalpy of Ge self diffusion in SiGe. It should be noted that while these activation enthalpy data sets are in reasonable agreement, the cited measurements of Q' differ by an order of magnitude.

Several strategies have been utilized to probe interdiffusion in SiGe alloys. Recent work has included thin sectioning with radio isotopes,[11,21] direct observation of concentration profiles by secondary ion mass spectrometry (SIMS)[1,10,19] and Rutherford backscattering spectrometry (RBS),[22,23] and measurements of superlattice evolution by both Raman spectroscopy[6,7] and x-ray diffraction (XRD).[2,4] The original studies of interdiffusion in SiGe were performed by thin sectioning with radio isotopes and were hampered by the need to work with polycrystalline bulk SiGe, limited depth resolution associated with mechanical sectioning techniques, and the short half life of Ge radio tracers. While these issues were largely overcome in a recent study by Strohm et al., the technique still provides no means of strain measurement during interdiffusion. Direct observation of concentration profiles has been the most commonly employed strategy. Proper interpretation of these measurements requires fitting calculated diffusion profiles to the measurements. To do this, the form of all concentration dependencies must be assumed *a priori*. Furthermore, SIMS yields no information on strain and RBS is hampered by a depth resolution of only five to ten nanometers for typical experimental geometries. X-ray diffraction measurements of the composition modulation in finely-structured superlattice films is certainly the most sensitive technique available[24] with the capability of directly measuring diffusion coefficients as low as 10^{-20} cm^2/s. The two great advantages of this method are that interdiffusion, strain, and structural characterization can be performed in a single experiment, and that interdiffusion is detected

directly. Therefore, assumptions about the form of concentration and strain dependencies are not required.

Once diffusion is measured, its interpretation can be difficult in a materials system that may undergo time dependent relaxation processes. The idea of scaling interdiffusion data to overcome this challenge and extract deeper information about the interdiffusion process was presented by Wu.[25] Wu described how temperature invariant diffusion requires a constant activation enthalpy. The value of such an activation enthalpy can be determined by scaling the annealing times for various temperatures to equivalent times at a single temperature using the scaling factor $\gamma(\Delta H_a, T)$.

$$\gamma(\Delta H_a, T) = \frac{\exp(-\Delta H_a/T_{original})}{\exp(-\Delta H_a/T_{new})} \tag{2}$$

Thus the activation enthalpy for interdiffusion can be determined by selecting a value for $\gamma(\Delta H_a, T)$ that collapses data from several temperatures onto a single curve. It is significant that this technique requires no assumptions about the functional dependencies of the interdiffusivity.

II Experiment

Both reduced pressure chemical vapor deposition (RPCVD) and ultra high vacuum chemical vapor deposition (UHVCVD) were used to prepare Si/SiGe superlattices for this study. The RPCVD samples were grown in an ASM Epsilon One Epitaxial Reactor at 625^{o}C in a 15 Torr, hydrogen ambient. Dichlorosilane and germane were used as growth gases. The UHVCVD samples were grown at 550^{o}C with silane and germane growth gases. Further details of the UHVCVD growth are published elsewhere.[26] The three superlattices examined

in this study had the following structures $[\mathrm{Si}\,13\,nm/\,\mathrm{Si}_{0.88}\,Ge_{0.12}10.5\,nm]_{10}$, $[\mathrm{Si}\,3\,nm/\,\mathrm{Si}_{0.82}\,Ge_{0.17}11\,nm]_{12}$, and $[\mathrm{Si}\,3\,nm/\,\mathrm{Si}_{0.88}\,Ge_{0.12}6\,nm]_{20}$. Because these films were grown directly onto (001) Si substrates, the SiGe layers were in biaxial compression and the Si layers were unstrained. To suppress roughening, each superlattice was terminated with a Si layer.[27] These wafers will be referred to as SL10, SL12, and SL20 and are shown in Fig. 1.

Structural characterization was performed by matching simulations to symmetric x-ray diffraction about the (004) reflection using the Philips Epitaxy software package. RBS was used to measure average Ge concentration. A high degree of crystallinity was confirmed by ion channeling measurements, which compare the backscattering yield from a sample oriented on a primary crystallographic direction to its yield at a random orientation. All three superlattices had a minimum yield ratio (χ_{min}) of less than 4%, which corresponds to ideal substitutionality and crystalline order. Using plan view transmission electron microscopy (TEM), the average as-grown misfit dislocation spacing was found to be greater than one μm for all three superlattices. Cross sectional TEM was used to confirm layer thickness and uniformity.

Samples of each superlattice were cleaved into pieces of approximately one cm square and annealed in a quartz tube furnace using an ultra high purity nitrogen ambient. The temperature range for annealing experiments, 795^{o}C to 895^{o}C, was selected because it provided interdiffusion rates that were not so slow as to yield no change in XRD measurements of composition evolution and not so fast as to be difficult to study accurately using tube furnace anneals.

Using a misfit relaxation analysis derived by Houghton,[28] wafers SL12, SL20, and SL10 were found to be 7.5, 6.5, and 3.5 times thicker than t_c, the thermodynamically modeled critical thickness for strain relaxation. In all cases, the individual SiGe layers within the Si/SiGe superlattice were subcritical. There are many kinetic barriers to strain relaxation in superlattice structures, and clearly all three films were in the metastable thickness regime under growth conditions. To confirm the strain relaxation that did occur during annealing could be attributed to formation of misfit dislocations instead of surface roughening or point defect annihilation, we measured the average dislocation spacing in a series of annealed samples from wafer SL12, the "most supercritical" of the superlattices. For a given mean dislocation spacing, $\langle S \rangle$, the degree of strain relaxation is given by $b/(2\langle S \rangle)$, where b is the Burgers vector of a 60^o misfit dislocation. In all cases, direct misfit dislocation counting via TEM plan view observations agreed with XRD measurements of strain relaxation to within 10%.

Superlattice x-ray diffraction studies were performed on the annealed samples with a standard two-circle diffractometer using a triple-axis geometry at beamline 2-1 of the Stanford Synchrotron Radiation Laboratory. Observations of the diffraction pattern in the vicinity of the (004) reflection as a function of interdiffusion annealing time were used to extract both the degree of strain relaxation and the interdiffusivity ($\tilde{D}$). Strain was determined from the position of the superlattice (004) film peak relative to that of the Si substrate peak. Because strain relaxation was found to be negligible in the as-grown films, film strain could be directly determined from the position of the (004) film peak. Strain measurements obtained from the 2-circle diffractometer at beamline 2-1 were confirmed by 4-circle x-ray diffraction studies using a sealed-tube x-ray source in the Stanford Geballe Laboratory for Advanced

Materials. Interdiffusion measurements were based on superlattice satellite decay rates. For a sinusoidal composition profile, the interdiffusivity is exactly proportional to the rate of superlattice satellite decay as a function of annealing time according to:[24]

$$\frac{d}{dt}\ln\left[\frac{I(t)}{I(0)}\right] = \frac{-8\pi^2}{\lambda^2}D_\lambda \tag{3}$$

Where I is the intensity of the superlattice satellite peak and λ is the bilayer period. In practice, this relationship is also commonly applied to superlattice samples that initially possess a near square-wave composition profile.[4] Although this relationship is derived for satellite peaks about the (000) reflection, it has been shown that the (004) satellites have a similar decay rate and are less sensitive to experimental setup and surface conditions.[29] To further isolate our measurements from issues related to the experimental setup, we normalized the satellite peak areas by the area of the corresponding (004) film peaks before computing I/I_o. Beam and sample drift were accounted for by rocking the θ angle through the (004) peak in very fine increments and performing a separate symmetric scan at each location in θ. A characteristic superlattice x-ray diffraction pattern is shown in Fig. 2. The Si substrate and SiGe film (004) reflections, positive and negative first order superlattice satellite peaks, and distinct finite thickness oscillations are clearly visible in the figure.

III Results

Superlattice satellite decay curves for the three superlattices are shown in Fig. 3. From equation (3), the slopes of these curves are directly proportional to the interdiffusivity. For wafers SL12 and SL20, the samples with higher Ge content, there is a clear non-linearity to the decay rate. This corresponds to the transition from a fast diffusing initial transient

regime, to a more slowly diffusing steady state condition. Wafer SL12 exhibits a short and long-time interdiffusivity value of $4.6 \pm 0.2 \times 10^{-17}$ cm^2/s and $4.6 \pm 2.8 \times 10^{-19}$ cm^2/s respectively. The corresponding values for wafer SL20 are $3.6 \pm 0.4 \times 10^{-18}$ cm^2/s and $3.5 \pm 1.8 \times 10^{-19}$ cm^2/s. There is no obvious non-linearity in the decay rate for wafer SL10, it exhibited a constant interdiffusivty of $2.3 \pm 0.6 \times 10^{-18}$ cm^2/s.

We applied temperature scaling to our superlattice satellite decay curves to extract the average activation enthalpy of the interdiffusion process. The collapsed $log(I/I_o)$ curves are shown in Fig. 4. The most successful collapse occurred with activation enthalpies of 4.7 eV, 4.8 eV, and 5.0 eV for wafers SL12, SL20, and SL10 respectively.

Strain relaxation measurements on wafer SL20 are shown in Fig. 5. Even at long annealing times, only about 4% of the misfit strain was relieved. The uncertainty in these results suggests that there is a statistical process governing the degree of relaxation in each sample. Because the individual SiGe layers are subcritical, homogeneous nucleation of a threading dislocation within the superlattice is unlikely. External sources such as surface scratches and/or substrate dislocations may, however, produce threading dislocations which span multiple bilayers in the supperlattice and can thus effect stress relaxation by glide. We believe that it is the statistics of such external sources that governs the extent of final relaxation observed in our samples. Similar trends were observed for wafer SL12 with a maximum relaxation of about 10% of the misfit strain. No discernible relaxation was observed for wafer SL10. Note that the maximum possible degree of strain relaxation is a temperature independent value, but several kinetic barriers prevent our superlattice samples from reaching full relaxation. Thus the quantitative dependence of strain relaxation on temperature is not obvi-

ous from our data. A simplistic curve fit was applied to the data for use in the interdiffusion simulations discussed later.

IV Discussion

The transient enhanced interdiffusivity was two orders of magnitude greater than the long time interdiffusivity in wafer SL12, one order of magnitude greater in wafer SL20, and non-existent in wafer SL10. Similarly, the average activation enthalpies required for good scaling were lowest in wafer SL12, and highest in wafer SL10. This suggests that both the interdiffusivity and the rate of change in interdiffusivity as a function of time are strongly correlated with the average Ge concentration of the films (13%, 12% and 5% for wafers SL12, SL20, and SL10, respectively.)

As a means of understanding the behavior observed in these experiments, we examined literature reports on the concentration and strain dependencies of interdiffusion with the intention of simulating the behavior observed in our experiments. A similar analysis was attempted by Schorer et al.[7] who used the concentration dependent activation enthalpy data of McVay et al.[11] and did not account for any strain dependence of $\mathcal{D}$.

Figures 6 and 7 show the activation enthalpy and exponential prefactor values for Ge diffusion as a function of Ge concentration obtained by McVay et al.[11] and Zangenberg et al.[10] Since the latter represents the most thorough, elegant measurement of the concentration dependence of Ge self diffusion in SiGe available, that data was used as the input for our calculations. The zero-concentration value of the curves is well known as it corresponds to Ge diffusion in the pure Si. The activation enthalpy and exponential prefactor of Si self

diffusion are $4.5 \pm 0.5\ eV$ and $530 \pm 250\ cm^2/s$.[12] While the concentration dependent activation enthalpy for SiGe interdiffusion is fairly well characterized, there is considerable scatter in the available prefactor measurements. Since both data sets show an exponentially decreasing prefactor, we assume the simple form –

$$Do = A_{Do} \exp(-B_{Do} X_{Ge}) \tag{4}$$

where *A* and *B* are empirical fitting parameters. This exponential dependence is possibly related to entropy effects.

In interpreting the experimental data, it is important to distinguish between the interdiffusivity and self diffusion coefficient as they are fundamentally different quantities. Experimental work involving direct observation of tracer diffusion profiles inherently probes Ge self diffusion while measurements of the evolution of the superlattice composition modulation probe interdiffusion. In SiGe, the two quantities are related by the Darken equation formulated in terms of the regular solution model –

$$\tilde{D} = (D_{Ge} X_{\mathrm{Si}} + D_{\mathrm{Si}} X_{Ge}) \left[1 - \frac{\alpha X_{Ge} X_{\mathrm{Si}}}{k_b T} \right] \tag{5}$$

where D_i is the tracer diffusivity in a given alloy, X_i is atomic fraction of element i, and α is the enthalpy of mixing coefficient for the alloy. The second set of parentheses on the right hand side contains the Darken term. In SiGe, it leads to a maximum variation in interdiffusivity of less than 10%, but it is easily included in our calculations. The first set of parentheses encloses the Kirkendall term. Neglecting this term amounts to assuming $D_{Ge} = D_{\mathrm{Si}}$. A strong argument can be made that the literature values for the activation enthalpies of the two species are equal to within experimental error. For example, the activation enthalpy

for Ge tracer diffusion in Si is sufficiently similar to that of self diffusion that Ge tracers are often substituted for Si in self-diffusion measurements.[11,30] Further, measurements of the activation enthalpies for diffusion of Si and Ge in pure Ge are also in agreement, with ΔHa(Si in Ge) >2.9 eV[31] and ΔHa(Ge self diffusion) = 3.1 eV.[32–34] Thus, neglecting the Kirkendall effect amounts to assuming that $D_{oGe} = D_{o\,\mathrm{Si}}$, which we do for convenience in the following simulations.

Compared to the concentration dependence, the strain dependence of $\tilde{D}$ is more difficult to quantify. As mentioned earlier, the activation enthalpy for diffusion should be linearly proportional to the biaxial strain with a proportionality constant typically referred to as Q'. To the best knowledge of the authors, there are only two existing measurements of Q' for SiGe where the strain and concentration effects were properly separated. The values of Q' published for compressive strain are 160 ± 40 eV/unit strain,[10] and 18 eV/unit strain.[20] The latter measurement is in agreement with a value calculated in recent *ab initio* simulations that predict a value of Q' = 16.8 eV/unit biaxial strain.[35] The actual value of strain will be a function of both the local Ge concentration ($\varepsilon = -0.042\, X_{Ge}$) and the degree to which misfit dislocations at the film/substrate interface relieve the lattice mismatch. The misfit dislocation mediated strain relaxation is a time dependent quantity that was characterized for each wafer, as described above, and illustrated for wafer SL20 in Fig. 5.

$$\varepsilon_{net} = -0.042\, X_{Ge} + \varepsilon_{dislocations} \tag{6}$$

It should be noted that gradient energy effects play a negligible role in this system because SiGe forms a nearly ideal alloy. The enthalpy of mixing coefficient is only 6500 J/mol.[36]

Following the regular solution treatment by Cahn and Hilliard, –

$$\tilde{D}_\lambda = \tilde{D}(1 + \frac{8\pi^2\kappa}{\lambda^2 fo''} + \frac{2\eta^2 Y_{UVW}}{fo''}) \quad (7)$$

where fo" is the second derivative of the Hemholtz free energy, λ is the bilayer period, κ is the concentration gradient energy, η is the linear expansion per unit composition change, and Y_{UVW} is the biaxial modulus. It can be shown that $\tilde{D}_\lambda$ deviates from $\tilde{D}$ by less than 5% for our samples and that this difference has a negligible concentration dependence.

Finally, we consider the effects of vacancy and interstitial mediation of the diffusion process. It is generally accepted that both vacancies and interstitials contribute to diffusion in bulk Si with vacancies controlling 60% to 80% of the overall process.[20,30,37] Similarly, it is well known that both Si tracer diffusion in Ge and Ge self diffusion are controlled exclusively by a vacancy mechanism.[13] The interdiffusivity in SiGe could be written as the sum of separate terms for the two point defect mechanisms. Each term would have a unique concentration and strain dependence and the degree to which each mechanism operated would depend on concentration. Most of the necessary data for such a calculation does not exist. Therefore, for the sake of making a workable model, we accept the assumption of Cowern et al.[20] that interstitial effects are negligible in low Ge concentration films. They argue that diffusion in pure Si, where interstitial effects have a reasonable contribution, is very slow compared to diffusion in the Ge-rich regions where vacancy mediated diffusion dominates. As for Q' having a different value for vacancies and interstitials, our superlattices were grown directly on a Si substrate; thus strain enhancement occurred almost exclusively in the biaxially compressed Ge-rich regions where vacancy mediated diffusion dominates.

We are left with the following equation for the interdiffusivity of our samples –

$$\mathcal{D} = A_{Do} \exp(-B_{Do} X_{Ge}) \left[1 - \frac{\alpha X_{Ge} X_{Si}}{k_b T} \right] \exp\left(\frac{-\Delta H_a}{k_b T}\right) \tag{8a}$$

$$\Delta H_a = \Delta H_a \left(X_{Ge}\right) + Q' \left(-0.042\, X_{Ge} + \varepsilon_{dislocation}\left(t\right)\right) \tag{8b}$$

Using these relationships, we solved Fick's second law numerically with a commercially available PDE solver. To simplify the numerical calculations, diffusion was calculated within a "superlattice cell." That is, a single bilayer period was treated instead of the entire superlattice. By centering the cell at the midpoint of a SiGe layer, boundary conditions of zero flux could be applied. After performing the calculations, several of these bilayer cells were joined together to form a complete superlattice profile. Because, in the kinematic approximation, the diffraction pattern of such a structure corresponds to the square of its spatial Fourier transform, a fast finite Fourier transform operation was applied to extract theoretical superlattice satellite intensity decay rates using equation (3). This approach neglects diffusion effects at the surface and loss of Ge into the substrate. Both effects are expected to be very small for the experimental conditions we have modelled.

Figures 8 and 9 show the simulation results applied to our model data. Curve fits used for the concentration dependent input parameters, ΔH_a and D_o, are shown in Figs. 6 and 10. A value of Q' = 19 eV/unit strain was used, consistent with the measurements of Cowern et al.[20] The model results were sensitive to the exact curve fit applied to the literature data and those fits were optimized to produce the best possible match to our three data sets. However, even rough fits to the activation and prefactor data produced model predictions that agreed with our

measurements in terms of qualitative trends and interdiffusivity values to the correct order of magnitude. We also attempted to fit our data using Q' values close to 160 eV/unit strain, as reported by Zangenberg et al.[10] The resulting model was deemed unphysical because the exponential prefactor was forced to decrease by seven orders of magnitude between 0% and 30% Ge concentration in order to achieve reasonable agreement with our experimental data. As shown in Fig. 7, literature values for the prefactor decrease by only two orders of magnitude over a similar concentration range.[10,11]

It is also informative to consider the calculated diffusion profiles themselves. Figure 8 shows the calculated evolution a "superlattice cell" in a simulated multilayer having the same structure as our wafer SL20. The Ge-rich region broadens at the expense of the Ge-poor regions and the Ge concentration profile retains a flat top and steep slope at the layer interfaces far longer than would be expected for sinusoidal decay of the local composition. This behavior is similar to experimentally observed Si/SiGe concentration profile evolution reported in the literature.[3,22]

The coupling of strain relaxation to interdiffusion is addressed in Fig 12. The effects of strain relaxation were isolated by reformulating the model with a concentration independent activation enthalpy and exponential prefactor. In a simulation where extremely large fractions of the misfit strain (up to 100%) were relieved on a time scale similar to that shown in Fig. 5, the strain effects alone decreased the calculated superlattice satellite decay rates by several orders of magnitude. However, when the same exaggerated strain relaxation trend was simulated using the full, concentration dependent model, it became clear that its effects on the satellite decay rates were discernible, but secondary to the concentration dependence

of $\mathcal{D}$.

V Conclusions

A combined experimental and modeling study of interdiffusion and simultaneous misfit stress relaxation in epitaxial Si/SiGe heterostructures has been performed. Experimentally, we observed a transient fast diffusion regime in asymmetrically strained, single crystal, $Si/Si_{0.83}Ge_{0.17}$ superlattices with overall average Ge concentrations of 12% and 13%. Transient fast diffusion was not observes however, in similar $Si/Si_{0.88}Ge_{0.12}$ superlattices with overall average Ge concentration of 5%. Clearly, the degree of enhancement was strongly correlated with the average Ge concentration of the Si/SiGe superlattice films. After being annealed for 25000 seconds at 870^{o}C, the films with 13% and 12% average Ge concentration exhibited an interdiffusivity change of two orders of magnitude and one order of magnitude, respectively. The film with only 5% average Ge concentration exhibited no clear change in interdiffusivity after the same thermal exposure.

We developed a model for SiGe interdiffusion based on literature reports of a SIMS experiment used to measure the activation enthalpy, exponential prefactor, and the strain dependence of Ge diffusion in SiGe. All model parameters were consistent with physical measurements and good agreement was found with the data reported in this study, which we obtained by an entirely different experimental strategy. The model is suitable for analysis of interdiffusion in asymmetrically strained, low concentration SiGe multilayers. However, there is no guarantee that the model parameters found to fit our data represent a unique solution, and thus they should be considered approximate. Despite these limitations, we conclude that

the Q' value on the order of 160 eV/unit compressive strain reported by Zangenberg et al. is clearly too large to be consistent with our experimental results. The Q' value reported by Cowern et al., of approximately 18 eV/unit biaxial strain, appears to be more realistic.

Using our model we have shown that the transient, fast initial interdiffusion often reported in Si/SiGe superlattices results primarily from the concentration dependence of the activation enthalpy of the interdiffusivity. While time-dependent strain relaxation was shown to contribute somewhat to the transition from fast to slow diffusion, it was found to be only a secondary effect. In the experiments reported here, strain did influence the overall diffusion rates, but made no significant contribution to the transition from fast to slow interdiffusion regimes.

This work was supported by the Department of Energy basic energy sciences grant DE–FG03–99ER45788.

[1] S. S. Iyer and F. K. Legoues, Journal of Applied Physics **65**, 4693 (1989).

[2] Baribeau, Appl. Phys. Lett. **57**, 1502 (1990).

[3] J. M. Baribeau, Journal of Applied Physics **74**, 3805 (1993).

[4] J. M. Baribeau, Journal of Vacuum Science and Technology B **16**, 1568 (1998).

[5] S. J. Chang and K. L. Wang, Applied Physics Letters **54**, 1253 (1989).

[6] S. M. Prokes, O. J. Glembocki, and D. J. Godbey, Applied Physics Letters **60**, 1087 (1992).

[7] R. Schorer, E. Friess, K. Eberl, and G. Abstreiter, Physical Review B **44**, 1772 (1991).

[8] Y. S. Lim, J. Y. Lee, H. S. Kim, and D. W. Moon, Applied Physics Letters **77**, 4157 (2000).

[9] S. M. Prokes and K. L. Wang, Applied Physics Letters **56**, 2628 (1990).

[10] N. R. Zangenberg, J. L. Hansen, J. Fage-Pedersen, and A. N. Larsen, Physical Review Letters **8712**, 5901 (2001).

[11] G. L. Mcvay and A. R. Ducharme, Physical Review B **9**, 627 (1974).

[12] H. Bracht, E. E. Haller, and R. Clark-Phelps, Physical Review Letters **81**, 393 (1998).

[13] A. Willoughby, J. Bonar, and A. Paine, Materials Research Society Symposium Proceedings **568**, 253 (1999).

[14] M. J. Aziz, Applied Physics Letters **70**, 2810 (1997).

[15] P. Kuo, J. L. Hoyt, J. F. Gibbons, J. E. Turner, and D. Lefforge, Applied Physics Letters **66**, 1293 (1995).

[16] P. Kringhoj, A. N. Larsen, and S. Y. Shirayev, Physical Review Letters **76**, 3372 (1996).

[17] A. N. Larsen and P. Kringhoj, Applied Physics Letters **68**, 2684 (1996).

[18] F. H. Baumann, J. H. Huang, J. A. Rentschler, T. Y. Chang, and A. Ourmazd, Physical Review Letters **73**, 448 (1994).

[19] N. E. B. Cowern, P. C. Zalm, P. Vandersluis, D. J. Gravesteijn, and W. B. Deboer, Physical Review Letters **72**, 2585 (1994).

[20] N. E. B. Cowern et al., Electrochemical Society Proceedings **96**, p 195 (1996).

[21] A. Strohm, T. Voss, W. Frank, J. Raisanen, and M. Dietrich, Physica B **308-310**, 542 (2001).

[22] G. F. A. Vandewalle et al., Thin Solid Films **183**, 183 (1989).

[23] B. Hollander, R. Butz, and S. Mantl, Physical Review B (Condensed Matter) **46**, 6975 (1992).

[24] A. Greer and F. Spaepen, *in Synthetic Modulated Structures, edited by L. Change and F. Giessen*, Academic Press, Orlando, 1985.

[25] D. T. Wu, in Crucial Issues in Semiconductor Materials and Processing Technologies, edited by S. Coffa, F. Priolo, E. Rimini, and J. M. Poate. , 403 (1992).

[26] P. M. Mooney and J. Chu, Annual Review of Materials Science **30**, 335 (2000).

[27] H. J. Gao and W. D. Nix, Annual Review of Materials Science **29**, 173 (1999).

[28] D. C. Houghton, Journal of Applied Physics **70**, 2136 (1991).

[29] S. M. Prokes, M. Fatemi, and K. L. Wang, Journal of Vacuum Science and Technology B (Microelectronics Processing and Phenomena) **8**, 254 (1990).

[30] P. Fahey, S. S. Iyer, and G. J. Scilla, Applied Physics Letters **54**, 843 (1989).

[31] J. Raisanen, J. Hirvonen, and A. Anttila, Solid-State Electronics **24**, 333 (1981).

[32] E. Silveira, W. Dondl, G. Abstreiter, and E. E. Haller, Physical Review B (Condensed Matter) **56**, 2062 (1997).

[33] H. D. Fuchs et al., Physical Review B (Condensed Matter) **51**, 16817 (1995).

[34] M. Werner, H. Mehrer, and H. D. Hochheimer, Physical Review B (Condensed Matter) **32**, 3930 (1985).

[35] R. Ramanarayanan and K. Cho, unpublished work (2002).

[36] T. B. Massalski, H. Okamoto, P. R. Subramanian, and L. Kacprzak, *Binary alloy phase diagrams*, 1990.

[37] A. Ural, P. B. Griffin, and J. D. Plummer, Journal of Applied Physics **85**, 6440 (1999).

Figure 1. D.B. Aubertine.
Journal of Applied Physics

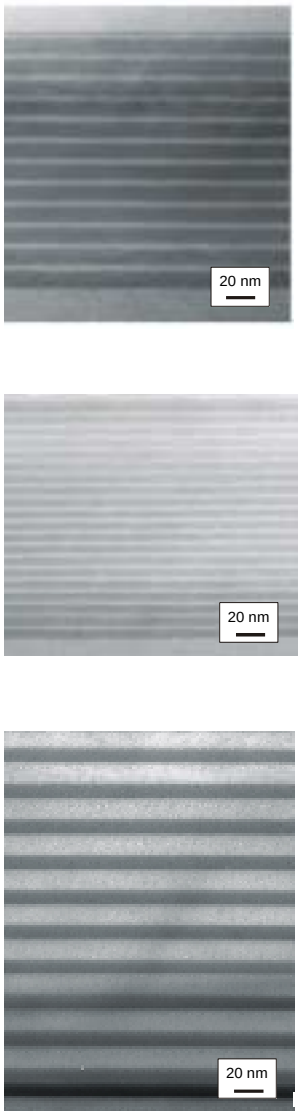

Fig. 1. Cross sectional TEM of (a) wafer SL12 with structure [Si 3 nm/$Si_{0.83}Ge_{0.17}$ 11 nm]$_{12}$. (b) wafer SL20 –[Si 3 nm/$Si_{0.83}Ge_{0.17}$ 11 nm]$_{20}$, and (c) wafer SL10 – [Si 13 nm/$Si_{0.88}Ge_{0.12}$ 11 nm]$_{10}$. Wafer SL10 had an unusually high Ge concentration at the film/substrate interface, this was not expected to have a significant effect on the interdiffusion.

Figure 2. D.B. Aubertine.
Journal of Applied Physics

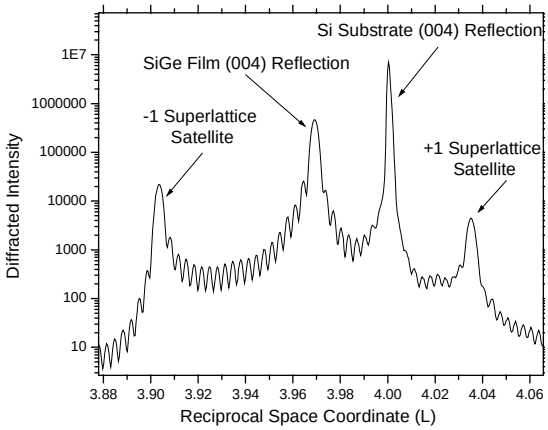

Fig. 2. Symmetric diffraction pattern of wafer SL20, as grown. Seven orders of dynamic range were typically available through the use of synchrotron source x-rays.

Figure 3. D.B. Aubertine.
Journal of Applied Physics

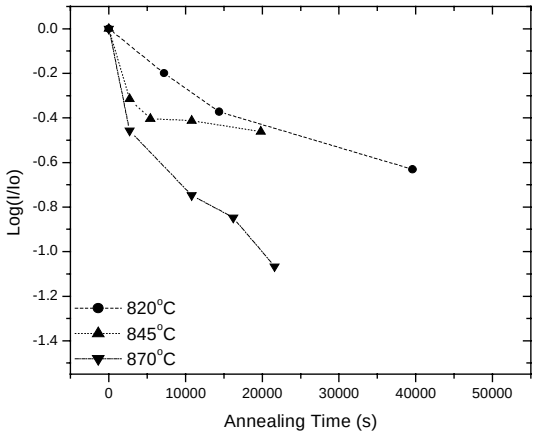

(a)

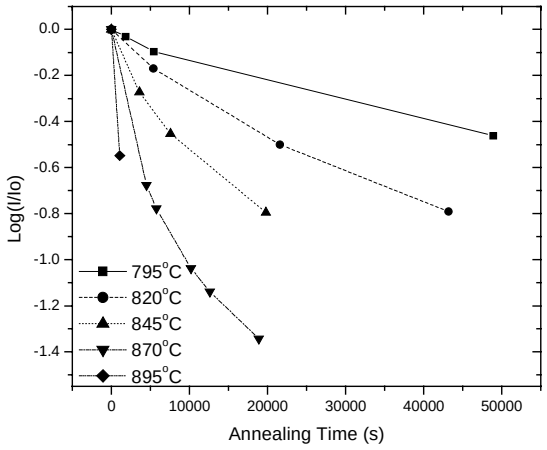

(b)

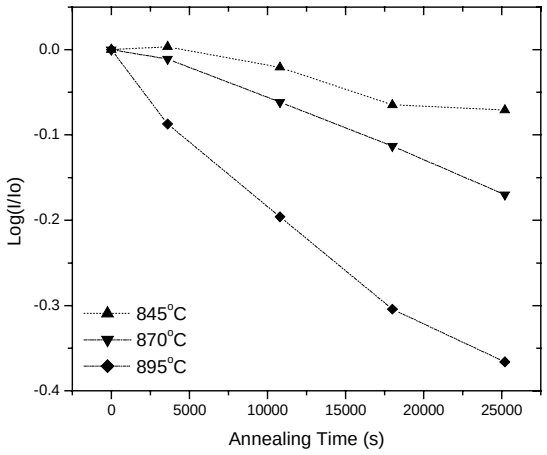

(c)

Fig. 3. Superlattice decay profiles for (a) wafer SL12, (b) wafer SL20, and (c) wafer SL10.

Figure 4. D.B. Aubertine.
Journal of Applied Physics

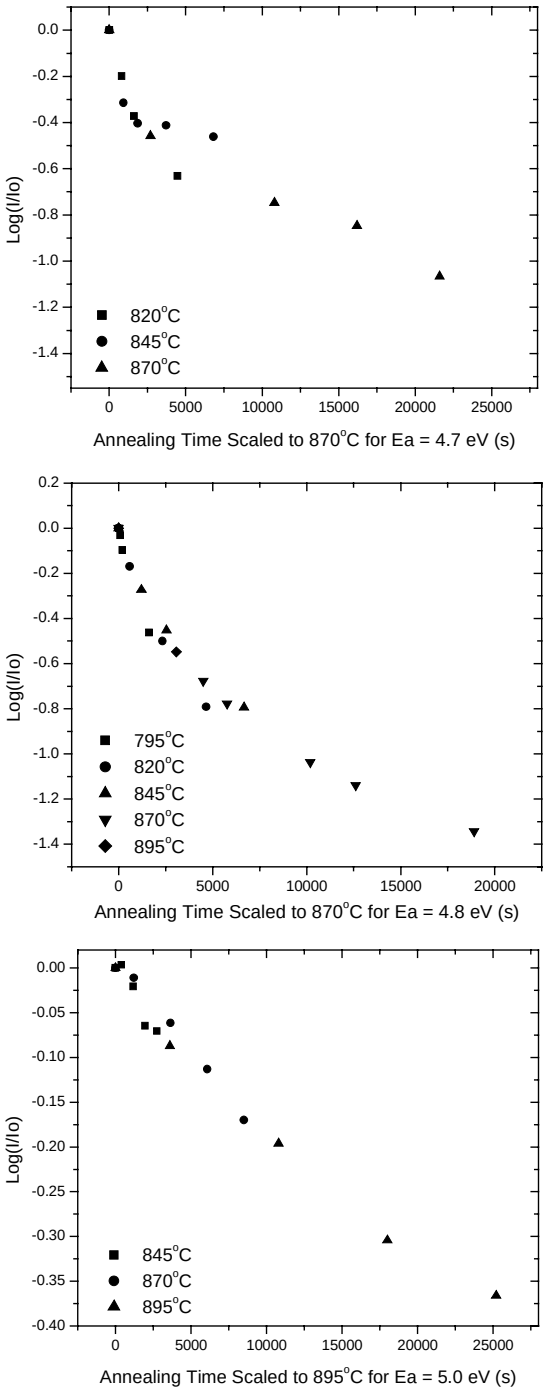

Fig. 4. Superlattice satellite decay rates scaled to determine the average activation enthalpy of the interdiffusion process. (a) Wafer SL12 scaled to equivalent annealing times at 870ºC, (b) wafer SL20 also scaled to 870ºC, (c) wafer SL10 scaled to 895ºC.

Figure 5. D.B. Aubertine.
Journal of Applied Physics

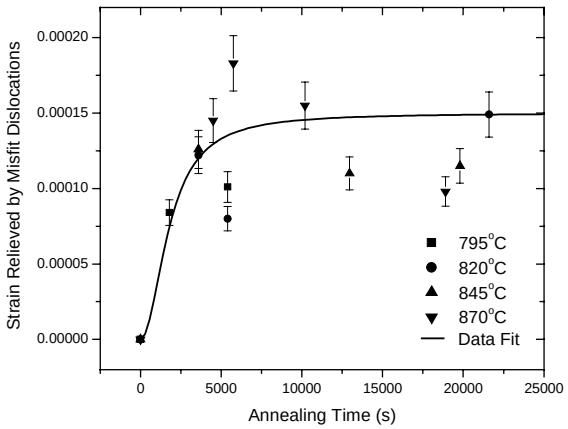

Fig. 5. Strain relaxation results for wafer SL20. The same general trend toward a maximum degree of strain relaxation was also observed for wafer SL12. An approximate curve fit was applied to the strain relaxation data for wafers SL20 and SL12 to facilitate numerical simulation of the diffusion process.

Figure 6. D.B. Aubertine.
Journal of Applied Physics

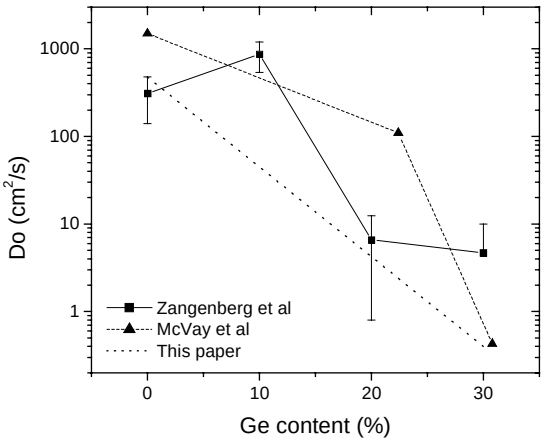

Fig. 6. Concentration dependent exponential prefactor for Ge diffusion in SiGe alloys. Results are shown from work by McVay and DuCharme,[11] Zangenberg et al,[10] and from the data fits obtained in this paper. All three data sets are consistent with well established values for the prefactor in pure Si.

Figure 7. D.B. Aubertine.
Journal of Applied Physics

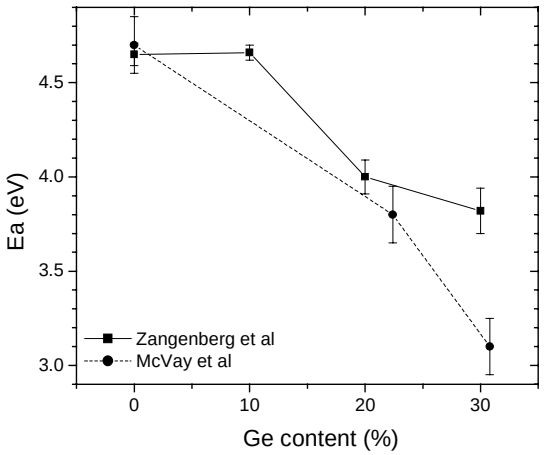

Fig. 7. Concentration dependent activation enthalpy for Ge diffusion in SiGe alloys. Results are shown from work by both McVay and DuCharme,[11] and Zangenberg et al.[10] Note that In the Zangenberg data set, the activation energy remains at a constant value from 0% to at least 10% Ge concentration.

Figure 8. D.B. Aubertine.
Journal of Applied Physics

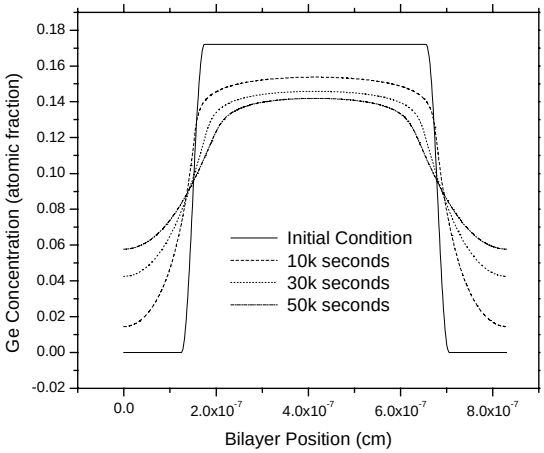

Fig. 8. Calculated annealing profile for a single supperlattice cell. The calculation was performed for wafer SL20 at 870°C. Higher diffusion rates in the SiGe region lead to expansion of the Ge rich region at the expense of the Ge poor regions. It is also interesting to note that rather than decaying to a sinusoid, the profile peaks retain on a broad, flat shape.

Figure 9. D.B. Aubertine.
Journal of Applied Physics

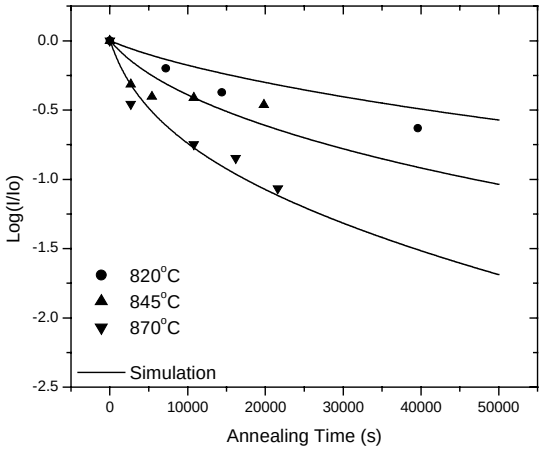

(a)

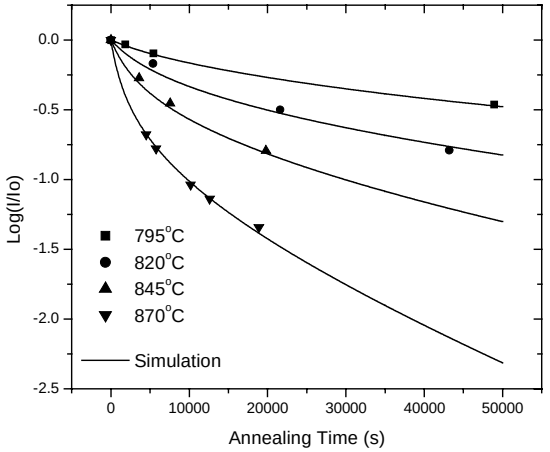

(b)

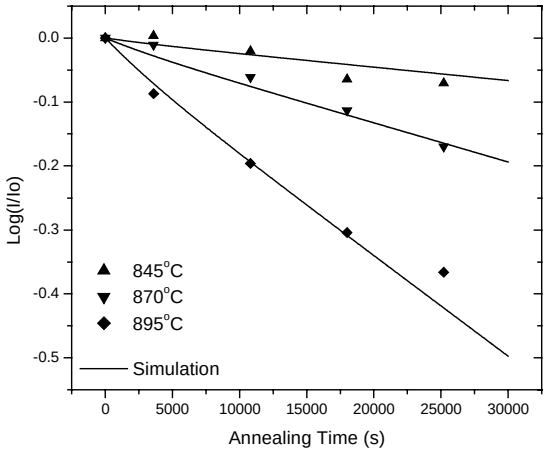

(c)

Fig. 9. Results of interdiffusion modelling plotted with the original data. Calculation parameters were Q' = 19 eV/unit strain, A_{Do} = 475 cm^2/s, B_{Do} = 20. a) wafer SL12, (b) wafer SL20, (c) wafer SL10.

Figure 10. D.B. Aubertine.
Journal of Applied Physics

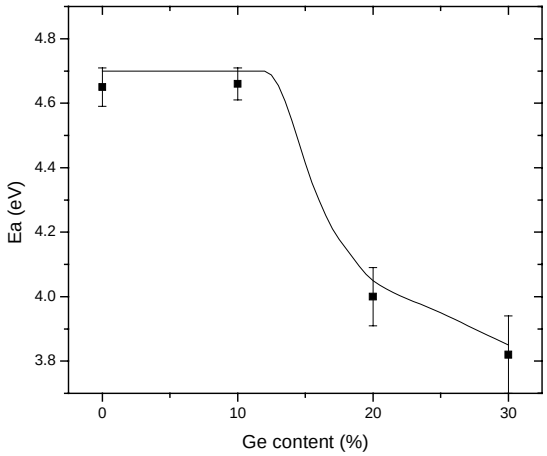

Fig. 10. The curve fit shown was applied to the activation energy reported by Zangenberg et al.[10] for the purpose of modeling diffusion in our system.

Figure 11. D.B. Aubertine.
Journal of Applied Physics

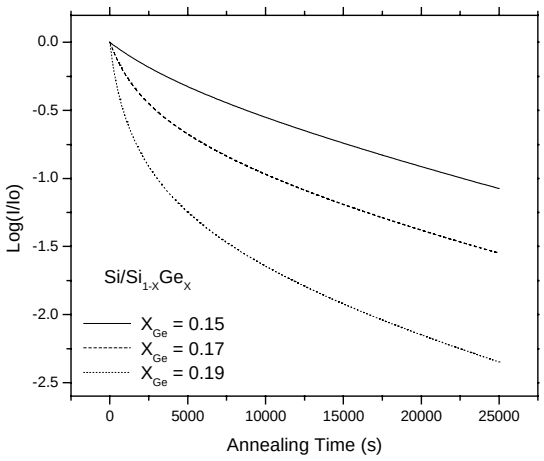

Fig. 11. Satellite decay rate simulations for a structure similar to that of wafer SL20 with increasing Ge concentration in the SiGe layers.

Figure 12. D.B. Aubertine.
Journal of Applied Physics

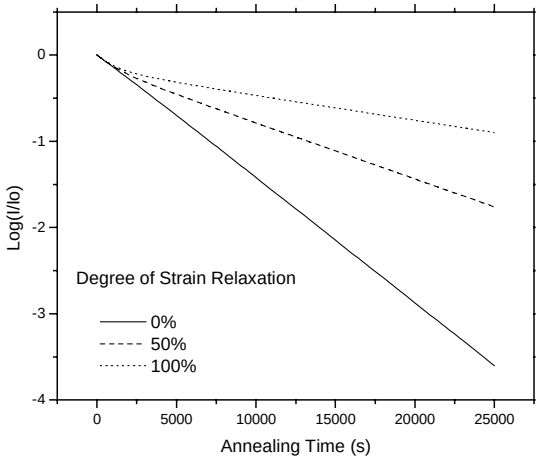

(a)

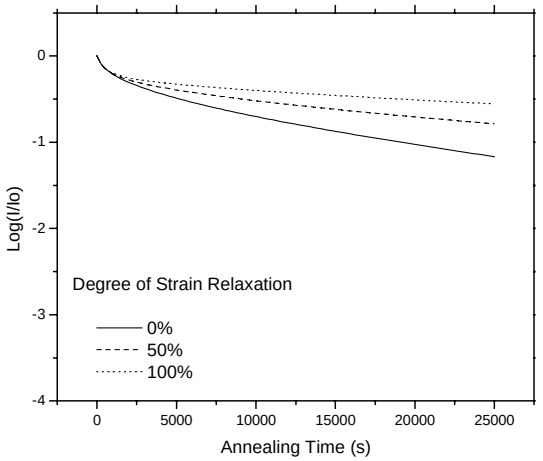

(b)

Fig. 12. Effect of strain relaxation on interdiffusion in a superlattice of the form [Si 2 nm/$Si_{0.8}Ge_{0.2}$ 6 nm]$_{20.}$ (a) Assuming the activation enthalpy and exponential prefactor remain at values appropriate for Si self diffusion, independent of concentration. (b) Assuming activation enthalpy and exponential prefactor vary with concentration in a manner consistent with measurements of Zangenberg et al.[10]